

Moisture origin and transport processes in Colombia, northern South America

I. Hoyos^{1,2}  · F. Dominguez³ · J. Cañón-Barriga¹ · J. A. Martínez⁴ · R. Nieto^{5,6} · L. Gimeno⁵ · P. A. Dirmeyer⁷

Received: 19 March 2016 / Accepted: 20 March 2017 / Published online: 9 April 2017
© Springer-Verlag Berlin Heidelberg 2017

Abstract We assess the spatial structure of moisture flux divergence, regional moisture sources and transport processes over Colombia, in northern South America. Using three independent methods the dynamic recycling model (DRM), FLEXPART and the Quasi-isentropic back-trajectory (QIBT) models we quantify the moisture sources that contribute to precipitation over the region. We find that moisture from the Atlantic Ocean and terrestrial recycling are the most important sources of moisture for Colombia, highlighting the importance of the Orinoco and Amazon basins as regional providers of atmospheric moisture. The results show the influence of long-range cross-equatorial flow from the Atlantic Ocean into the target region and the role of the study area as a passage of moisture into South America. We also describe the seasonal moisture transport

mechanisms of the well-known low-level westerly and Caribbean jets that originate in the Pacific Ocean and Caribbean Sea, respectively. We find that these dynamical systems play an important role in the convergence of moisture over western Colombia.

Keywords Colombian climate and variability · Atmospheric moisture transport processes · Recycling and terrestrial moisture sources · Oceanic moisture source

1 Introduction

Atmospheric transport processes play a primary role in the study of continental-scale interactions among the components of the hydrologic cycle. These interactions regulate the life cycles and the transfer of ecosystem services—even between remote locations (Wagener et al. 2010; Jackson et al. 2001), exerting an important control on biodiversity, water availability and management of resources.

In tropical areas, moisture flux convergence and the seasonal migration of the Inter Tropical Convergence Zone (ITCZ) largely control the general climate traits. However, in northern South America, especially over Colombia, the regional moisture transport processes are driven by the confluence of global and local factors. Contributing factors include the topographic split of the Tropical Andes, the proximity to the Caribbean Sea and Pacific Ocean, the trade winds, Tropical Easterly Waves (TEWs), El Niño—Southern Oscillation (ENSO), Atlantic Multidecadal Oscillation (AMO), and Pacific Decadal Oscillation (PDO), among others (Durán-Quesada et al. 2012; Garreaud 2009; Poveda et al. 2006). In spite of its dynamic complexity, the study of climatic and hydrologic processes in this region has a short history and constitutes

✉ I. Hoyos
isabel.hoyos@udea.edu.co

¹ Facultad de Ingeniería, Grupo GAIA, Universidad de Antioquia, SIU/UdeA, Calle 70 N 52-21, Medellín, Colombia

² Instituto de Física, Grupo de Fundamentos y Enseñanza de la Física y los Sistemas Dinámicos, Universidad de Antioquia, Medellín, Colombia

³ Department of Atmospheric Sciences, University of Illinois at Urbana-Champaign, Champaign, USA

⁴ Department of Atmospheric Sciences, University of Arizona, Tucson, USA

⁵ EPhysLab (Environmental Physics Laboratory), Facultad de Ciencias Universidade de Vigo, Ourense, Spain

⁶ Department of Atmospheric Sciences, Institute of Astronomy, Geophysics and Atmospheric Sciences, University of São Paulo, São Paulo, Brazil

⁷ Center for Ocean-Land-Atmosphere Studies, George Mason University, Fairfax, VA, USA

an open area of research (Garreaud 2009; Célleri and Feyen 2009).

Topography plays an important role in atmospheric transport processes because orographic flows strengthen the formation of rainfall patterns, that in turn are fed by convective mesoscale fluxes (Bhushan and Barros 2007; Roe 2005; Lin et al. 2001). The orographic complexity of Colombia makes it difficult for numerical models to accurately represent the spatial and temporal details of regional climate variables such as precipitation and temperature (Hoyos et al. 2013b; Buytaert and Bièvre 2012). In addition, there is a scarcity of accessible meteorological gauge information for scientific use (Durán-Quesada et al. 2012).

López and Howell (1967) were among the first to explore the relationship between regional physiography and transport processes. They proposed a conceptual description of atmospheric flow and convective system formation over the western Colombian Andes based on the application of the heated hydraulic jump theory, and showed that relative cool air flow from the Pacific Ocean produces circulation patterns that modulate local climate regimes. Poveda and Mesa (2000) defined a low-level westerly jet system (CHOCO jet) with seasonal development that could explain the existence of one of the rainiest places in the world (Lloró, Colombia), in an important ecoregion characterized by large biodiversity and biotic connectivity (Bass et al. 2010). Some of the major regional hydro-climatic controls are studied in Poveda et al. (2006) from intra-seasonal to inter-decadal time scales, identifying the Caribbean and Pacific low level jets, convective mesoscale systems and potential Amazon-Andes feedback as important mechanisms, that along with the ITCZ, partially control the regional spatial variability of climate and precipitation regimes. In terms of regional atmospheric moisture contributions, Sakamoto et al. (2012) explored the moisture sources related to convective systems for westernmost Colombia during 2003 by tracking the evolution of cloud clusters and finding their source of moisture with the FLEXPART method. They found a significant prevalence of Mesoscale Convective Systems (MCS) originating in continental areas in comparison to those that originated in marine regions with a broad monthly distribution of moisture sources. However, the Tropical North Atlantic and The Peruvian-Chilean Pacific show a permanent source of moisture for the regional MCS through the year. Arias et al. (2015) ranked the percentage of multiannual precipitable water contributions from 20 different regions for the the anomalous 2010–2012 wet season in northern South America, using the Dynamical Recycling Model. They found that moisture from Atlantic Ocean, local recycling and terrestrial recycling from Amazon and Orinoco Basins are the most important regional sources of moisture.

In this study, we present a regional description of the climatological characteristics of the study area using the ERA-Interim reanalysis (Dee et al. 2011). This dataset has been found to provide a reliable representation of the atmospheric component of the hydrological cycle (Lorenz and Kunstmann 2012; Trenberth et al. 2011). Furthermore, some of the climate and orographic features in the Colombian region are better captured in this dataset compared with the performance of some previous reanalyses such as ERA-40 and NCEP/NCAR (Hoyos et al. 2014; Hoyos et al. 2013b). A detailed description of seasonal advance of precipitation and moisture flux divergence and their relationship with regional topography is presented in Sect. 2, including the identification of an orographic passageway in the Ecuadorian Andes, transporting moisture from Amazon Basin to Equatorial Pacific area. In Sect. 3, the dominant moisture sources over the region are delimited and their corresponding regional contributions are quantified using three independent and complementary approaches from different models. Differing from previous studies (Arias et al. 2015; Sakamoto et al. 2012; Poveda et al. 2006), the present one is not limited to a specific transport mechanism or an anomalous event. This study captures the most robust characteristics of the moisture source regions in a long-term perspective for the annual cycle, summarizing the large variability of moisture sources in northern South America as a key region in the intra-Americas atmospheric transport. Discussion and conclusions are presented in Sect. 4.

2 Regional rainfall and atmospheric moisture

Due to its proximity to the Equator, the Colombian territory is exposed to quasi-constant incoming solar radiation throughout the year. Consequently, convection is one of the most relevant short timescale atmospheric processes and the range of variation in the temperature annual cycle is smaller than the range of variation in the diurnal cycle. The seasonality is mainly defined by the annual regime of precipitation, which spatially varies in agreement with the migration of the ITCZ. The Pacific Ocean and the Caribbean Sea, which constitute the country's western and northern boundaries respectively, have strong influence on Colombian climate and make the region sensitive to coupled global climatic phenomena such as: Tropical Easterly Waves (TEWs) that primarily influence northern Colombia (IDEAM 2005); the North Atlantic Oscillation (NAO), which also impacts the northern part of the country, as can be seen through significant changes in river discharge (Mesa et al. 1997). El Niño—Southern Oscillation (ENSO) is perhaps the ocean–atmosphere coupled phenomenon of greatest importance in Colombian climate, whose effects

are felt throughout the country, with large consequences for the population and water/energy resources. The warm phase of ENSO generally brings lower than average precipitation, increases air temperature and is therefore associated with a higher probability of drought. In contrast, the cold phase of ENSO brings above average precipitation with increased river discharges and landslide occurrences. The ENSO phases have been associated with extreme hydroclimate events in the country (Hoyos et al. 2013a). During El Niño, there is an increase in forest fires, crop losses, fish population reduction and a deficit in hydroelectric energy supply. Conversely, La Niña events are characterized by increasing flood risks, erosion issues, and infrastructure damages (Pabón 2003; Waylen and Poveda 2002; Carvajal et al. 1998).

Within the Colombian territory, the Andean mountain chain is divided into three branches, which in turn divide the country into four basins: Caribbean, Pacific, Orinoco and Amazon (Figure 1). The factors mentioned above result in the large spatial and temporal variability of Colombian climate that is barely represented in earlier generations of reanalysis (ERA-40 and NCEP-NCAR) as reported in Hoyos et al. (2013b). Atmospheric moisture and precipitation are key variables in the representation of regional climate processes. These variables account for the accumulated effect of hydrological processes in the Colombian basins and modulate the life cycles of a great variety of ecosystems within the territory (Myers et al. 2000).

In this section, precipitation and atmospheric moisture are evaluated as indicators of the hydrological cycle representation in the reanalysis ERA-Interim. In this data set, many of the problems in tropical areas have been

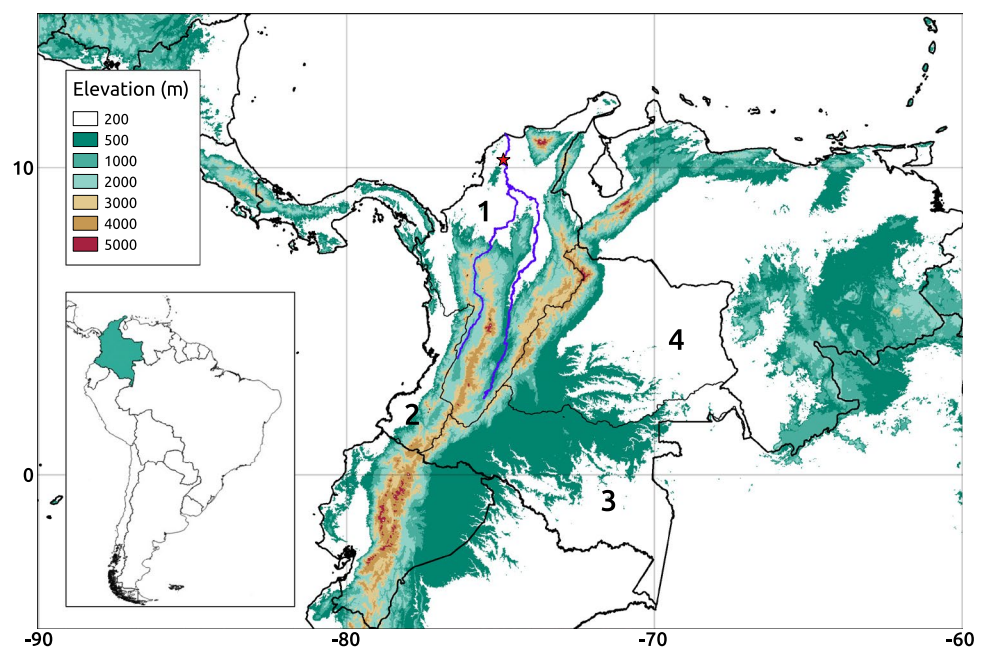
minimized, especially the closure of hydrological cycle and over-estimations in precipitation and moisture transport of previous ECMWF reanalyses (Dee et al. 2011).

2.1 Performance of regional rainfall in ERA-Interim data

The regional rainfall in the study area is modulated by the annual cycle of ITCZ and its interaction with topography, producing a distinct seasonal cycle of precipitation for different regions across the territory, therefore, a description in terms of the major Colombian basins (see Fig. 1) is more suitable because of the quasi-homogeneous shape of the annual cycle of precipitation (bimodal or unimodal) in each one of these large catchments (IDEAM 2005; Pabón et al. 2001; Mesa et al. 1997; Eslava 1994; Snow 1976).

The Caribbean and Pacific basins are characterized by a bimodal annual cycle with the rainiest periods in March, April and May (MAM) and September, October, November (SON) while the Amazon and Orinoco basins have a unimodal cycle with maxima in May and June respectively. Figure 2 compares the annual cycle from observational data with respect to precipitation from Tropical Rainfall Measuring Mission (TRMM) and ERA-Interim data. The spatial structure of precipitation is shown for representative months (Fig. 3), where data reported in the Climatology Atlas of Colombia from rain gauge data (IDEAM 2005) are also included. Qualitatively, regional processes are well represented by ERA-Interim data, highlighting the continuously high rainfall regime in the northern part of the Pacific catchment, the low rainfall regime in the northern Caribbean

Fig. 1 Study area. Regional orography (m) from Global Land One-kilometer Base Elevation (GLOBE, (Hastings and Dunbar 1998)). Colombian Catchments delimited in black line: 1 Caribbean, 2 Pacific, 3 Amazon and 4 Orinoco. Cauca and Magdalena major rivers in Caribbean Catchment in blue line. Red star marks the Magdalena river flow sampling point



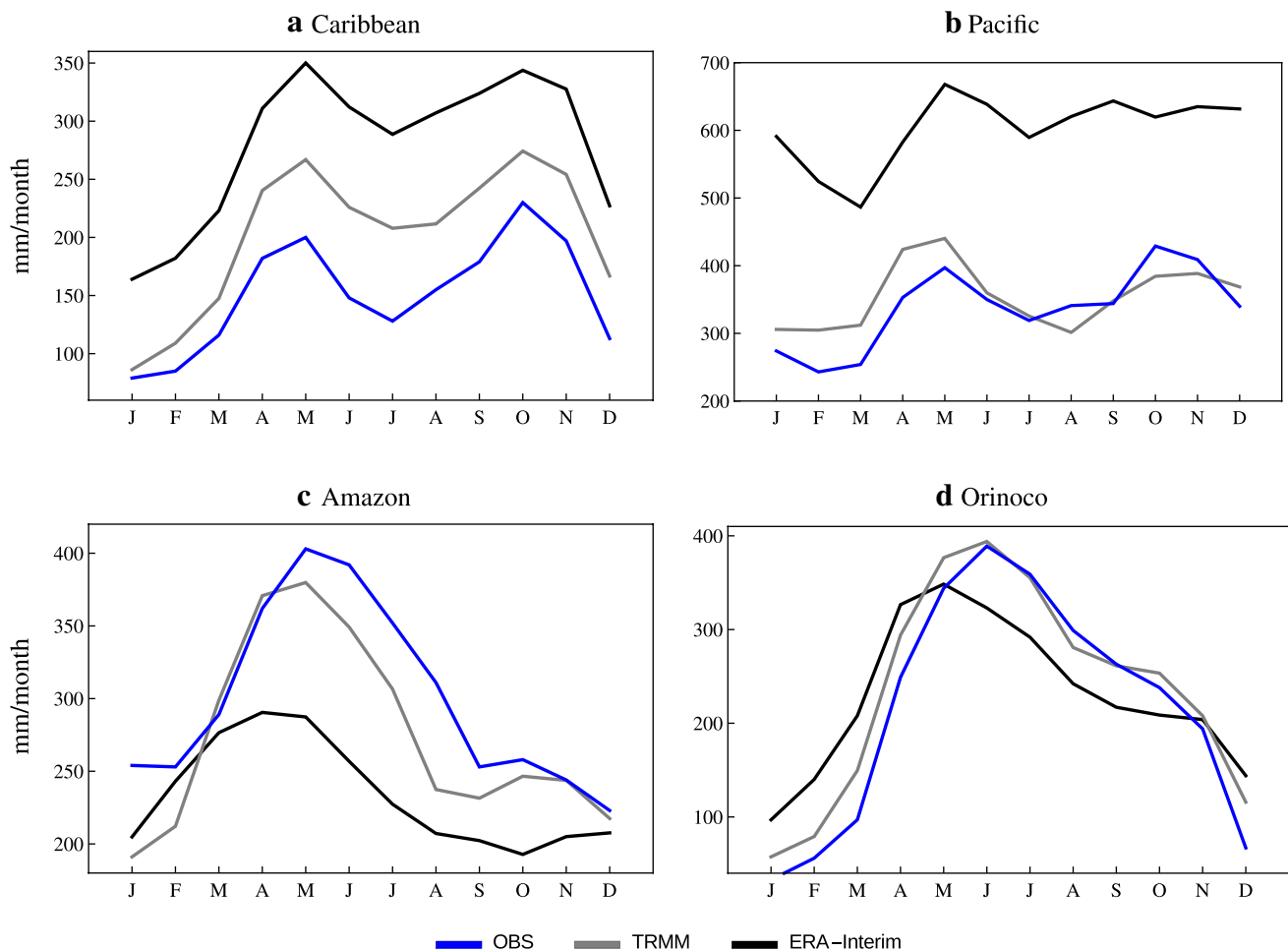


Fig. 2 Annual cycle of precipitation in the Colombian basins. Source data from gauge stations provided by the Instituto de Hidrología, Meteorología y Estudios Ambientales (IDEAM)—OBS, the Tropical Rainfall Measuring Mission—TRMM and the ERA-Interim reanalysis

catchment, the spatial variability of precipitation in the Colombian Andean ranges and the spatial homogeneity in the Colombian Orinoco and Amazon Catchments, as described in IDEAM (2005), Pabón et al. (2001) and Snow (1976).

In agreement with observations, both TRMM and ERA-Interim describe the main characteristics of the annual cycle in each Colombian basin. However, ERA-Interim overestimates the precipitation amount over the Caribbean and Pacific basins (85 and 78%, respectively). These are the regions with larger orographic complexity and spatial variability in the country. On the contrary, ERA-Interim underestimates the precipitation amount over the Amazon basin by an average of 22% (ranging from only 5% during February and March to 75% during May and June), and the rainy season begins one month in advance. In the Orinoco catchment, the precipitation amount is more realistic (with an overestimation of only 6%), but the maximum in the rainy season is one month before observations. A summary of

average precipitation in each one of Colombian catchments is presented in Table 1.

In the ERA-Interim reanalysis, precipitation is a model-generated variable (Dee et al. 2011). Its accuracy largely depends on the quality of the model physics, which could explain the generalized bias in the rainfall amount. On the other hand, observations of the Total Column Water Vapour (TCWV) are assimilated (since August, 1987) over oceanic areas from microwave imagery and soundings, whereas humidity over land is observationally constrained. The assimilation of oceanic observations indirectly affects ERA-Interim's precipitable water in this terrestrial region through the 4D-Var assimilation. Despite very few radiosonde observations are available for this region (see Uppala et al. 2005), data assimilation from satellite images are substantially increased since 1989 (Dee et al. 2011). Therefore, a coherent field representation of precipitable water is expected during the TCWV assimilation period in this reanalysis (Dee et al. 2011; Tavolato and Isaksen 2010;

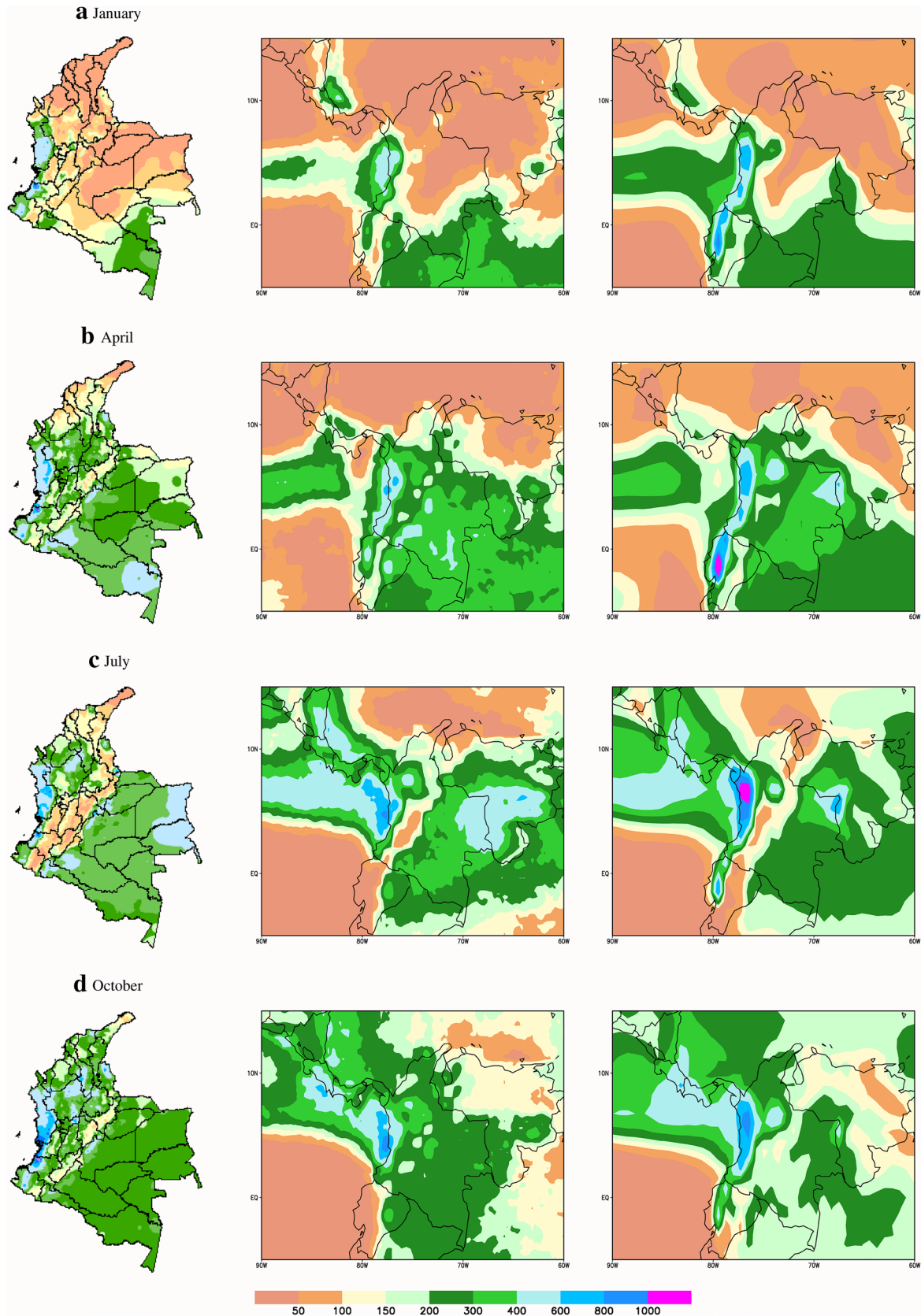


Fig. 3 Regional precipitation (mm/month) for seasonal representative months. Data from IDEAM (2005) (*left*), Tropical Rainfall Measuring Mission TRMM (*center*) and ERA-Interim (*right*). Colors and value ranges fitted to IDEAM (2005) scale for comparison purposes

Table 1 Summary of annual average of regional precipitation (in mm/month)

Colombian catchment	Observations	TRMM			ERA-Interim		
		Average	SD	Bias (%)	Average	SD	Bias (%)
Caribbean	151	188	73	34	300	218	85
Pacific	338	328	128	5	554	187	78
Amazon	299	272	29	-9	233	28	-22
Orinoco	215	233	30	9	238	74	6

Andersson et al. 2005; Uppala et al. 2005). TRMM only provides precipitation related data and it is not possible to obtain the moisture flux fields studied in our paper. For these reasons, we focus our attention in the assessment of atmospheric moisture in ERA-Interim.

The Colombian Caribbean basin is the only one that meets the three following criteria: (1) it is entirely contained within the Colombian territory, (2) Its geomorphology makes the Magdalena River a good hydrological integrator (the gauge station is located at the rivers outlet and accounts for the whole discharge, as it is shown in Fig. 1), and (3) the available time series for the Magdalena River discharge (see Fig. 4) has a period long enough to guarantee the closure of the surface water balance (Hartmann 1994). These criteria allow us to use the river discharge as an independent variable to evaluate the accuracy of the regional representation of the climatology in ERA-Interim. By contrast, the Orinoco and Amazon basins fail to satisfy the first criteria and the Pacific Colombian catchment does not satisfy the last two.

Despite the significant bias of precipitation amount in the ERA-Interim data over the Caribbean catchment and the secular shifts in the ERA-Interim precipitation behavior, especially in the early 2000s because of changing sources of satellite data used for assimilation (Geer et al. 2008), the monthly variability of total precipitation (in terms of standardized anomalies as suggested by Hoyos et al. (2013b), for data with a generalized bias) closely follows the basin runoff, summarized by the Magdalena

river discharge in the basin (Fig. 4a). We also review the seasonal relationship between precipitable water and river flow as a hydrological closure property (Fig. 4b). Due to the thermodynamic relationship between precipitation and precipitable water, together with the observational constraint of precipitable water in ERA-Interim (Dee et al. 2011; Andersson et al. 2005), a qualitative correspondence between the annual cycle of precipitable water and runoff in the Magdalena river basin is expected, with some characteristic hydrologic response lag associated with the size of the basin. A Pearson correlation of $r = 0.43$ (p value $< 1\%$) between standardized anomalies of discharge and precipitable water from ERA-Interim for the period 1980–2013 is an indication that anomalies dynamically represent the variability in this region. The annual cycle of river discharge exhibits a bimodal regime controlled by the ITCZ migration with 1-month response lag with respect to total precipitable water cycle.

2.2 Regional moisture processes

As expected in tropical areas with low-level convergence and high surface temperature, the moisture convergence follows the rainfall patterns. This seasonal spatial patterns of vertically integrated Moisture flux divergence (MFD, from ERA-Interim) are presented in Fig. 5. The MFD in the inter-Andean region, the portion of the Caribbean basin dominated by the Tropical Andes, is highly sensitive to the ITCZ stages, with moisture divergence

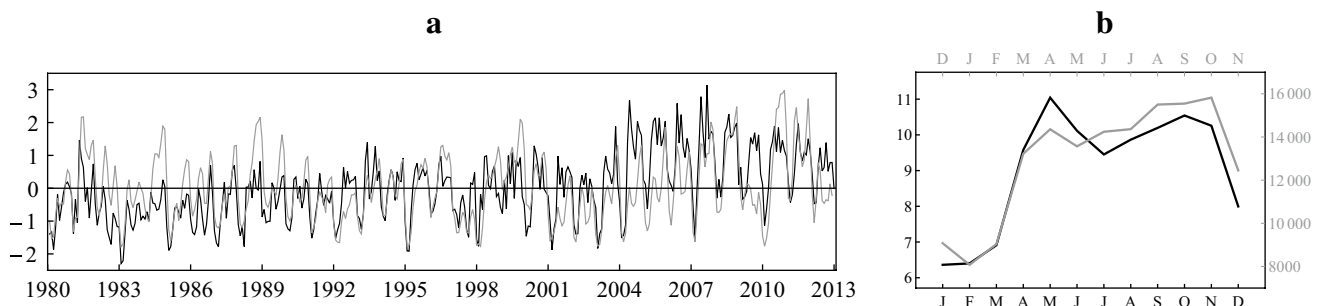


Fig. 4 Hydrology in the Caribbean catchment basin. **a** Standardized anomalies of Magdalena river discharge (gray, lagged 1 month) and monthly precipitation from ERA-Interim. **b** Annual cycle of total

precipitable water from ERA-Interim (black, in mm) and Magdalena river discharge (gray, in mm^3/s) with 1-month response lag

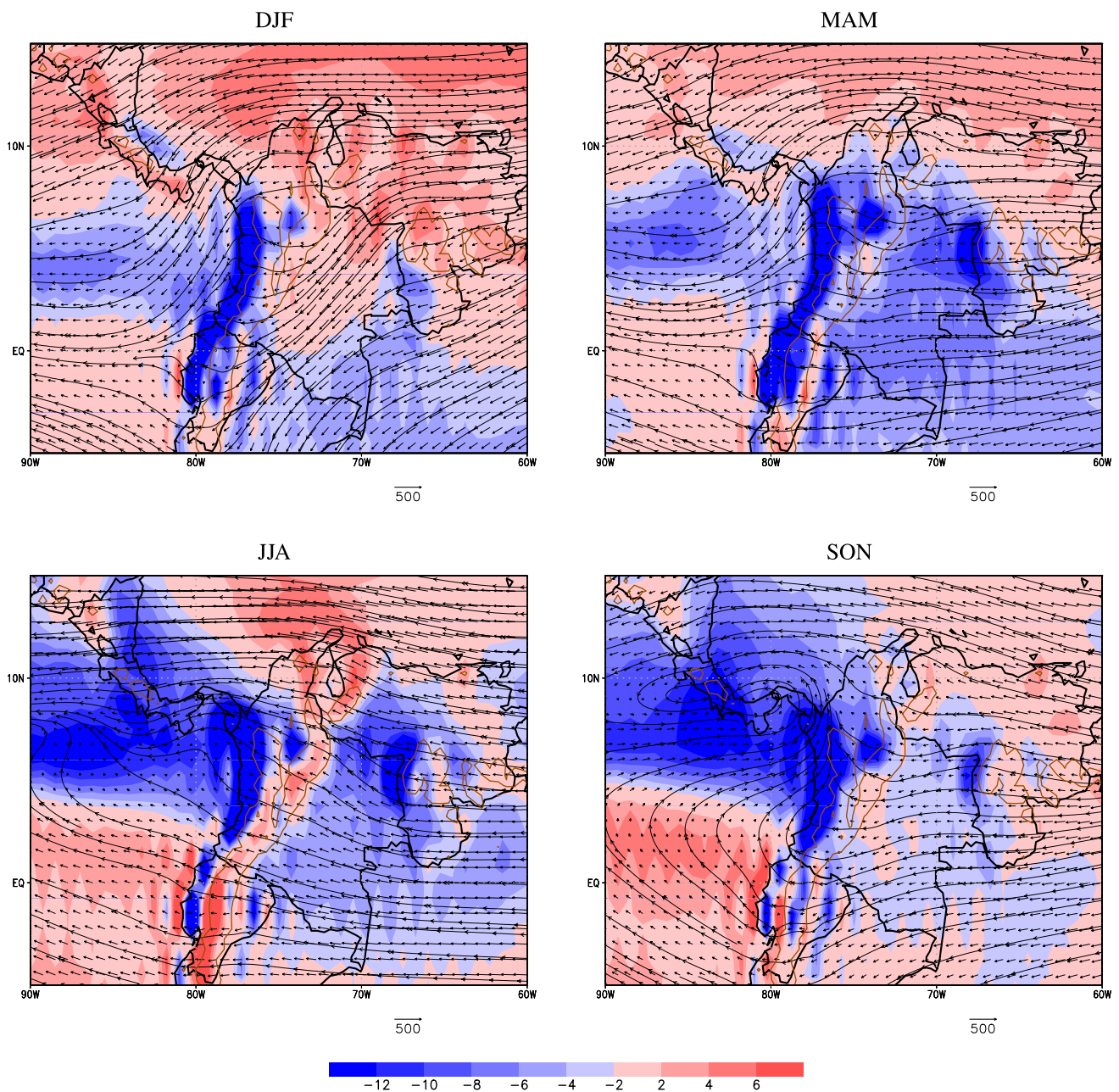


Fig. 5 Seasonal moisture flux divergence (mm/day) in background. Vertical water vapor flux vector field ($\text{kg m}^{-1} \text{s}^{-1}$). Brown contour line corresponds to 1 km elevation

during the dry seasons December, January and February (DJF) and June, July and August (JJA) and moisture convergence during the rainy seasons (MAM and SON). Moisture in this area is composed by seasonal differential contributions from local and remote terrestrial sources and the oceans. Some of this moisture leaves the country in the form of Mesoscale Convective Systems that travel to the ocean and precipitate over the northern part of the Colombian Pacific basin (see Sakamoto et al. (2012) and Mapes et al. (2003)). A permanent orographic moisture

convergence zone centered around 7°N , 74°W can be distinguished.

The Pacific catchment is a permanent convergence zone throughout the year, due to moisture contributions from the North Atlantic and West Pacific oceans. These contributions change their intensity during the year in agreement with the seasonal cycle of the low level transport from the Caribbean and the Pacific (as we discuss below). From December to May (Fig. 5a, b), the eastern flank of the Andes blocks the predominant easterly

moisture flux, diminishing the moisture that crosses over the Andes. Simultaneously, the flow further north the Andes crosses northern Colombia and experiences an accelerated southward deviation over eastern Central America and Tropical Pacific, trapping moisture over western Colombia. During JJA (Fig. 5c), the regional flow lines experience an increase in the northern component, producing a convergence area that extends from western Colombia to Central America. In SON season (Fig. 5d), the vertically integrated moisture transport from the Pacific Ocean reaches the Pacific Colombian catchment, whereas the western flank of the Andes works as an orographic barrier, which results in a significant excess of moisture in this zone. The easterly flux in the meantime is stalled over the western Andes due to a combination of an orographic blocking and a circulation pattern blocking over the Pacific Ocean (López and Howell 1967).

Over the Orinoco and Amazon catchments, the ITCZ advances slower than over the rest of the country. This behavior produces a unimodal convergence of moisture with maximum in MAM (Fig. 5b). The dry season (DJF, Fig. 5a) occurs when the ITCZ is at its southernmost location and the regional orography deflects the easterly moisture flux southward. A strong northeasterly flux crosses through the Orinoco and Amazon basins causing localized weak moisture convergence over this area. At the same time, the Caribbean catchment has dry conditions because the East Andean range works as an orographic barrier that diminishes the incoming moisture flux into the inter-Andean portion of the basin.

As the ITCZ advances to higher latitudes, the interaction between the Tropical Easterly Winds and the mountain range weakens and then there is an increase of convergence and an enhancement of convective processes (IDEAM 2005). Both, the Caribbean low-lands and the inter-Andean region show moisture convergence in the first rainy season (MAM) and almost the entire country is an atmospheric moisture sink. During the second dry season JJA, when the ITCZ is at its northernmost location, the inter-Andean region shows moisture divergence while the rest of the territory has moisture convergence. During the second rainy season, the north-western region has strong moisture convergence due to contributions from the Pacific Ocean, only present during this season, whereas the south-eastern part of the country has weak moisture convergence. Notably, an orographic passageway located south of the study area, characterized by a decrease of the average elevation in the Andes around 5°S, 78°W (Montgomery et al. 2001), is likely working as a channel of moisture transport from the eastern flank of the Andes to Pacific Ocean to strengthen the convergence in western Colombian coast, as shown in Figs. 5 and 6. Figure 6 shows the zonal mean of moisture flux over the portion of Tropical Andes with heights greater than 500 m. The blocking effect of mountains varies in accordance with the average elevation and the atmospheric level pressure. At lower atmospheric levels (950 hPa) there is low zonal transport across the Tropical Andes which increases as pressure level decreases, in such a way that zonal moisture flux crossing across the Tropical Andes has a non-negligible component at higher pressure levels. The zonal moisture flux has a negative peak in the orographic

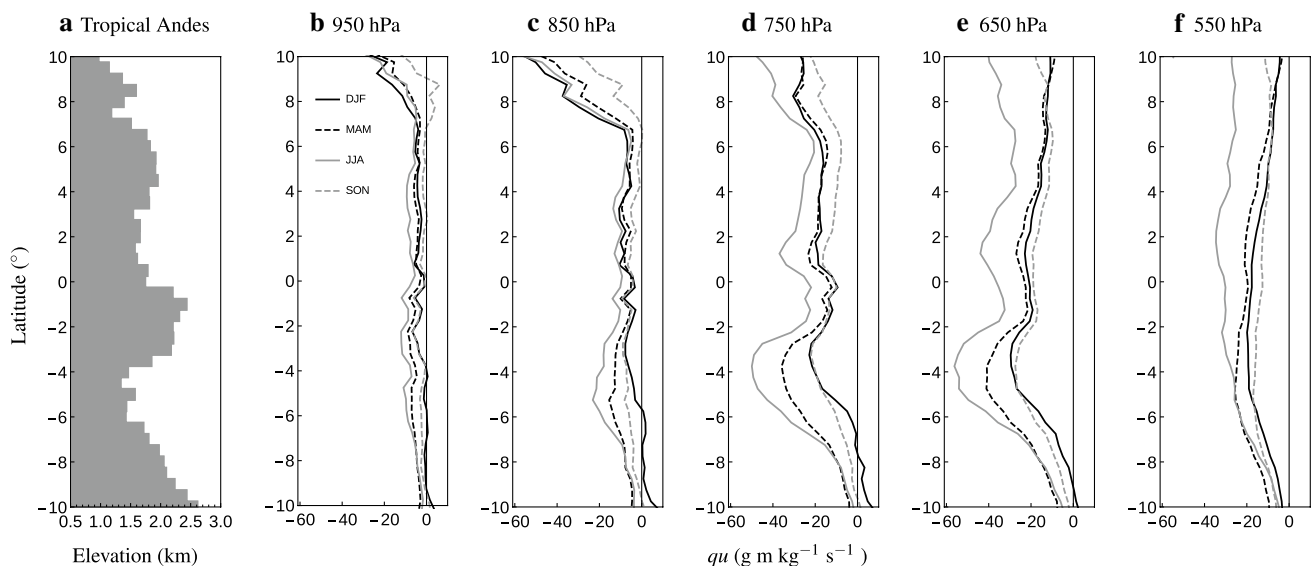


Fig. 6 Zonal mean of total moisture flux over the portion of Tropical Andes with heights greater than 500 m. **a** Mean Elevation of Tropical Andes. Zonal mean of moisture flux at **b** 950 hPa, **c** 850 hPa, **d** 750 hPa, **e** 650 hPa and **f** 550 hPa. Data source: ERA-Interim

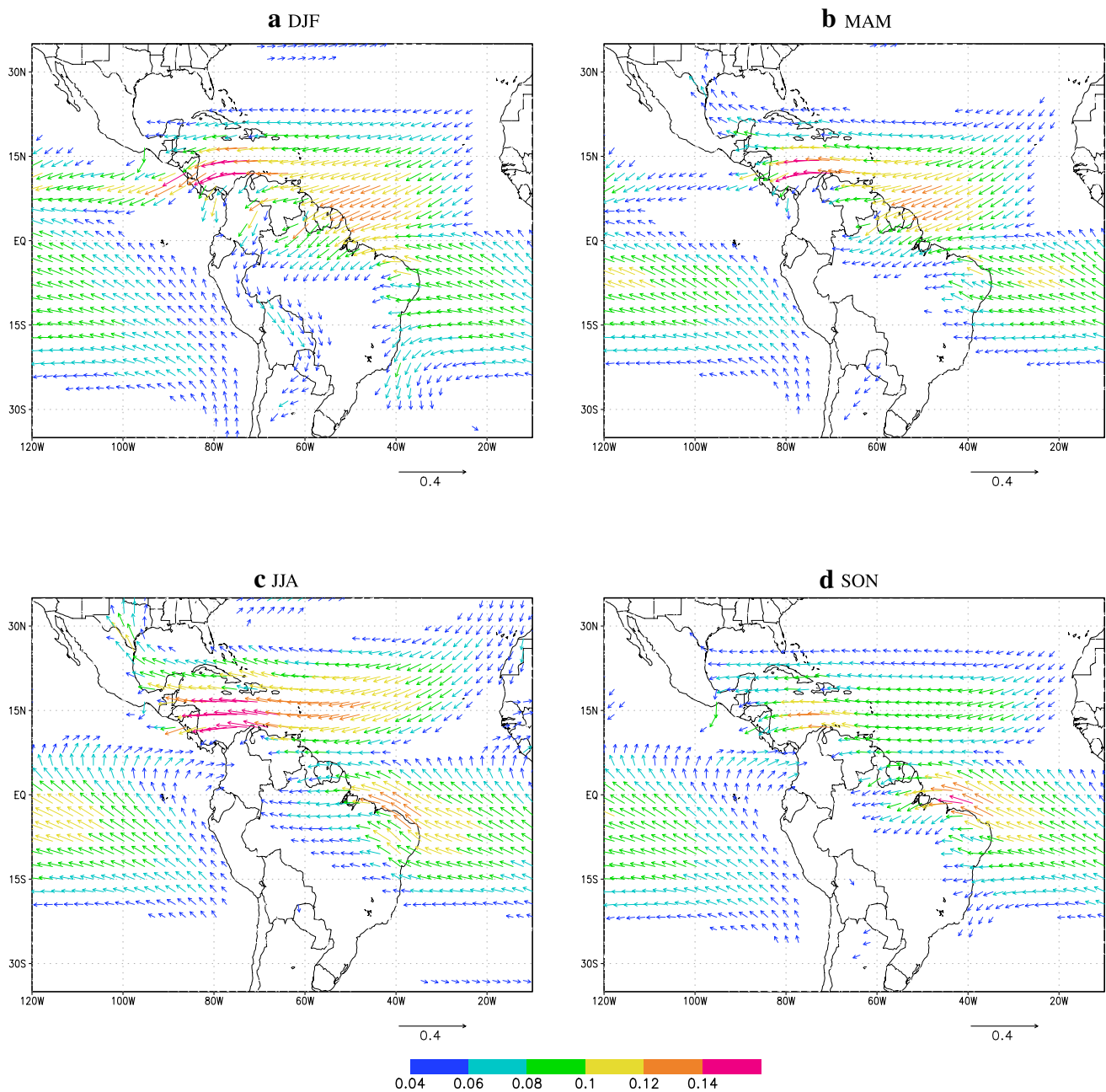


Fig. 7 Seasonal moisture flux field at 925 hPa ($\text{kg m}^{-1} \text{s}^{-1}$), from ERA-Interim reanalysis

passageway around 5°S with a maximum in SON season, indicating a contribution to atmospheric moisture from the east that crosses the Andes and flows to the Pacific Ocean.

Regional moisture transport by low level jet systems from the Caribbean Sea and the Pacific Ocean has been widely recognized (Poveda et al. 2014; Sakamoto et al. 2012; Poveda et al. 2006). Figure 7 shows the seasonal structure of low level moisture flux from ERA-Interim data product. The regional low level westerly jet, commonly known as CHOCO Jet, is an important regional moisture

transport mechanism feeding the Colombian Pacific Basin, one of the rainiest regions in the world (Poveda and Mesa 2000). This structure begins its development during boreal summer, when the easterlies are in their northernmost location over Central America and the anticyclonic structure of the South Pacific High is extended northwards. The cold moist air coming from the Pacific Ocean is stalled over the western Colombian coast around 5°N with a maximum development during October. The Caribbean Low Level Jet (CLLJ, Amador (2008), Wang (2007), and Muñoz et al.

(2008)) is a permanent easterly zonal wind at 925 hPa with a bimodal cycle: with one maxima in the boreal summer (July) and another in the boreal winter (February). This annual cycle responds to sea level pressure changes in the North Atlantic Subtropical High (NASH) and its east-west excursion throughout the year (Wang 2007; Wang and Lee 2007). Its regional influence is mostly felt at the end of the SON season, when the blocking effect of the CHOCO Jet over the Tropical Pacific is weakened and the southward component of low-level transport is intensified when the ITCZ is in its southernmost position. As a result, the low level transport that crosses Central America deflects towards western Colombia, enhancing the moisture convergence in this area (seen in DJF). Also during this season, the moisture reaching Colombia on the eastern flank of the Andes experiences a southward acceleration of the meridional component due to the ITCZ location but also driven by the spatial configuration of the eastern branch of the Andes.

3 Sources of regional moisture and transport processes

3.1 Quantifying the regional moisture contributions

In this section we quantify the origin of moisture contributions to Colombia from terrestrial and oceanic areas through complementary approaches from three different backward trajectories models: the Dynamical Recycling Model DRM, the Quasi Isentropic Back-Trajectory (QIBT) and the Lagrangian particle dispersion model FLEXPART. DRM and FLEXPART use input data from ERA-Interim while QIBT uses NCEP/DOE input (Kanamitsu et al. 2002) and a hybrid precipitation data set described in Dirmeyer and Brubaker (2007). Features of each model are summarized in Table 2.

The DRM is a computationally efficient two-dimensional semi-Lagrangian model that provides moisture contributions from predefined source regions for a target region. This model is based on the moisture conservation equation for an atmospheric column in a semi-Lagrangian framework where the temporal changes in the vertical integral of water vapor for a moving atmospheric column are produced by P and E relationship $dW/dt = E - P$. In order to differentiate between local sources (i.e. from E in the

bottom of the air column) and external sources (accounting for the portion of W originated elsewhere), the model includes the classical assumption that the water vapor from different sources is well-mixed in the column (Burde and Zangvil 2001). Dominguez et al. (2006) found an analytical solution for the amount of moisture from local origin and Martínez and Dominguez (2014) extended this solution to estimate contributions from local and remote sources by tracking how much moisture is collected from different regions along their back-trajectories which are followed until they exit the domain.

In the QIBT model, the precipitation events in a 5-day temporal window trigger the backward moisture tracking. The exact starting positions of tracked parcels are randomly fixed within a grid box in the horizontal and initial elevation is defined probabilistically by the vertical distribution of moisture in the tropospheric column. Each parcel is tracked backward on an isentropic surface no more than 15 days and the model quantifies the evaporative source along the track supplying precipitation to the target region, assuming that the fraction of precipitable water is due to uniformly mixed surface evaporation in the atmospheric column in each time step of the backward trajectory (Dirmeyer and Brubaker 2007; Dirmeyer and Brubaker 1999).

FLEXPART—the most complex model included in this study—is based on a 3D Lagrangian dispersion model (including sub-grid turbulence and large scale convection, Stohl et al. (2005)) that fills the atmosphere with a large number of air particles (about 2 millions) that adopt the properties of physical system, so the position of each particle at a later time is determined by the fluids dynamical evolution. The trajectory of each particle located in the target region is followed backward as far as 10 days, considered the mean life time of water vapor in the atmosphere (Numaguti 1999). FLEXPART accounts for the net loss or gain of specific humidity (q) along a large number of trajectories. Temporal differences in q vertically integrated over a given area provides the $E - P$ relationship, where E and P are evaporation and precipitation respectively (Stohl and James 2004). The FLEXPART can be used in backward or forward mode, initializing the model over a target region and tracking trajectories backward or forward in time. Unlike the DRM and QIBT models, precipitation and evaporation are not directly separable in the FLEXPART model (Stohl and James 2004). However, regions where

Table 2 Summary of features of the moisture tracking models

Model	Grid	Data source	Period	References
DRM	241 × 480	ERA-Interim	1980–2012	Dominguez et al. (2006)
QIBT	192 × 94	NCEP/DOE	1980–2004	Dirmeyer and Brubaker (2007)
FLEXPART	360 × 180	ERA-Interim	1980–2012	Stohl and James (2004)

$E - P < 0$ represent moisture loss (precipitation exceeds evaporation in those areas), and $E - P > 0$ represent moisture gain (evaporation exceeds precipitation).

To reach a more consistent description among seasonal moisture contributions accounted by the three models, we ran an additional FLEXPART experiment in which we selected the most important regional moisture sources and used a forward simulation to obtain the net moisture received (or lost) in our target region of interest (Colombia) from each of these moisture source regions within a 10-day transport time. Hence, in this study we use both backward and forward approaches to compare with DRM and QIBT.

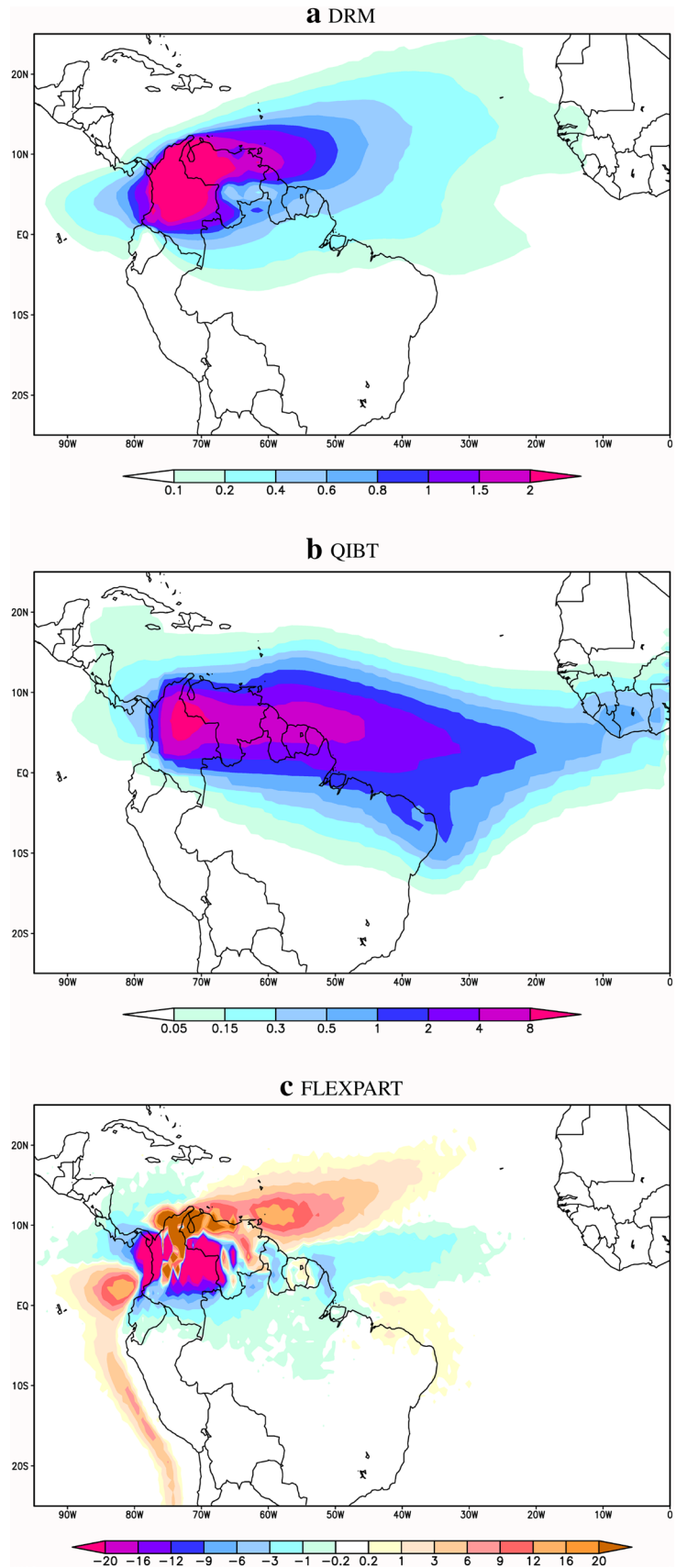
The target region is located in the northernmost part of South America (hereafter NOSA) and includes the Colombian inter-Andean region, the Caribbean low-lands and the Pacific Basin (see Fig. 1). As we discussed in Sect. 2, this area is directly affected by the influence of this mountain range in several ways, i.e. blocking the incoming flows, accumulating moisture in some specific areas, permitting the formation of orographic passageways that connects flows from different origins, among others. This is the most densely populated area in Colombia, where more than 80% of the population resides and where the major agro-industry development is located. The same target area is used in FLEXPART and DRM experiments, and is slightly smaller in QIBT. In QIBT, the target area corresponds to the Magdalena basin in the catalog of moisture sources for the World basins in the project Characterizing Land Surface Memory to Advance Climate Prediction (<http://www.iges.org/wcr/>).

Climatological maps (Fig. 8) present an indicator of spatial moisture contributions to NOSA for each model. The variables mapped for each model are different. For DRM (Fig. 8a) we map the variable $R_{gc} = \varepsilon \exp^{-(\varepsilon/\omega) \times t} \delta t$, which is an indicator of how much moisture comes to NOSA from each grid cell, according to the exponential solution used by the DRM model (Dominguez et al. 2006; Martínez and Dominguez, 2014), where ε and ω are the evaporation and precipitable water in each grid cell within the integration time δt . For the QIBT model, the climatological map is the most straightforward to interpret and corresponds to the amount of evaporated moisture from each grid cell that supplies precipitation over NOSA in a monthly scale. In FLEXPART, the climatological map shows the moisture sources, using 10-day integrated of net $E - P$ from backward trajectories. In the FLEXPART map, warm colors represent regions of net moisture gain and cool colors represent regions of net moisture loss. The three maps show agreements and differences among the three models. Contributions from the Tropical Atlantic are present in the three models. DRM and FLEXPART capture contributions as far as the Subtropical North Atlantic, while the QIBT shows the oceanic contributions concentrated in the Tropical

Atlantic, reaching western Africa. In QIBT and DRM moisture from the Pacific Ocean is limited to the adjacent marine region while FLEXPART exhibits long-range contributions from the Tropical South Pacific. Terrestrial sources are important contributions in the three models, and extend over the northern Amazon Basin. Based on this climatological description we selected the regions that potentially contribute to our target region (Fig. 9). Terrestrial sources correspond to the main hydrological units and oceanic regions are delimited in agreement with sources generated by FLEXPART. This choice allows us to account for the moisture transport processes associated with atmospheric circulation patterns and for terrestrial processes related to evapotranspiration from terrestrial basins. The terrestrial and oceanic source regions are defined as follows: Northern South America (NOSA); Subtropical North Pacific (STNP); Tropical North Pacific (TNP); Tropical South Pacific (TSP); Subtropical North Atlantic (STNA); Tropical North Atlantic (TNA); Tropical Atlantic (TA); Tropical South Atlantic (TSA); United States (US); Central America; Gulf of Mexico; Caribbean Sea (CARS); Orinoco Basin (ORIC); Guyanas (GUYN); Western Portion of Ecuador, Perú and Chile (PECH); Northern Amazon Basin (NAMZ); Southern Amazon Basin (SAMZ); Tocantins Basin (TOC); Northeastern Brazil (NEB); La Plata River Basin (LPRB) and Africa.

The main moisture sources of the study region and their relative influence are summarized in Table 3. According to DRM and QIBT, more than 80% of total moisture contribution comes from the Atlantic Ocean, Terrestrial sources and Adjacent Tropical Pacific. In both models, the biggest contribution comes from Tropical Atlantic (49 and 52%, respectively), followed by terrestrial sources with 30.4 and 32.5%, while Pacific Ocean contributions are below 3% in both models. The FLEXPART results of $E - P$ are obtained from the forward integration, only for those areas identified as source regions for NOSA in the climatological map (Fig. 8c) and assuming the total moisture contribution comes from these regions. This means that in this estimate, the regions classified as Others, the Gulf of Mexico and the Southern Tropical North Pacific are not accounted for in the forward FLEXPART simulation. FLEXPART shows negative values of $E - P$ for all contributing regions, that means the trajectories reaching NOSA from these remote areas lose moisture by an excess of precipitation over evaporation, diagnosing net precipitation. In agreement with Stohl and James (2004), summing $E - P < 0$ over a longer period (33 years in this case) leads to estimate the time average of diagnostic precipitation \bar{P} . In contrast to the DRM and QIBT results, the Adjacent Tropical Pacific is the biggest source of moisture providing 36.5% of precipitation in NOSA, while the Atlantic sources account for 25.5% (almost one half of that is accounted by DRM and

Fig. 8 Climatology of moisture contributions to NOSA as it is represented by **a**. DRM, the fraction of evaporation reaching NOSA from each grid cell (R_{gc} , mm), **b** QIBT, evaporated moisture that precipitates over NOSA (mm/month) and **c** FLEXPART, $E-P$ (mm/day) in backward mode. For FLEXPART, the net $E-P$ brings information about moisture lost or gain of particles along trajectories. Cold/warm colors are used to indicate that particles loss/gain moisture across their trajectories



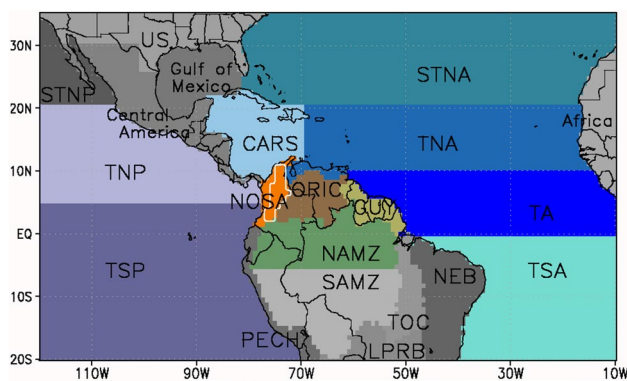


Fig. 9 Hydrographic units considered in the experimental setting for the DRM, QIBT and FLEXPART models. Northern South America (NOSA, target region), Subtropical North Pacific (STNP), Tropical North Pacific (TNP), Tropical South Pacific (TSP), Subtropical North Atlantic (STNA), Tropical North Atlantic (TNA), Tropical Atlantic (TA), Tropical South Atlantic (TSA), United States (US), Central America, Gulf of Mexico, Caribbean Sea (CARS), Orinoco Basin (ORIC), Guyanas (GUY), Western Portion of Ecuador, Perú and Chile (PECH), Northern Amazon Basin (NAMZ), Southern Amazon Basin (SAMZ), Tocantins Basin (TOC), Northeastern Brazil (NEB), La Plata River Basin (LPRB) and Africa. Target region in QIBT model is constrained to Magdalena river basin, slightly smaller than NOSA (white contour line). Regions with relevant moisture contributions to NOSA in color (gray tones for regions that contribute with less than 0.5% of annual mean of precipitable water)

QIBT). As in DRM and QIBT, terrestrial sources are also important in FLEXPART, accounting for 38% of average precipitation with a noticeable bigger contribution from recycling (NOSA, 17%, almost twice that reported by DRM and QIBT). We highlight the importance of terrestrial recycling from the Orinoco and Northern Amazon basins as well as local recycling over NOSA.

The time of maximum contribution depends on the distance from the source region and the strength of advective processes and precipitation-generating mechanisms, so the residence time of water vapor substantially changes between source regions. In DRM and QIBT the time of moisture contribution is determined by the location of trajectories and contributions from a region are only accounted while the backward trajectory is within a source domain, whereas in FLEXPART we have adopted 10 days that is the average residence time in the atmosphere (Numaguti 1999).

Figures 10, 11 and 12 show results of the three models for Atlantic, Pacific and terrestrial contributions, respectively. The units of the three models are different, so we present one unified graph with three y-axes to emphasize the seasonal cycle. For DRM we report precipitable water contributions, for QIBT we report the evaporative source supplying rainfall, and for FLEXPART we report the net loss of moisture over NOSA ($E - P < 0$). Although the model response variable is different in all models, it is

Table 3 Climatological percentage summary of moisture contributions to NOSA from local and remote sources as accounted by DRM, QIBT and FLEXPART models

Source	Region	DRM Precipitable water (%)	QIBT Evaporative source (%)	FLEXPART Diagnostic precipitation (%)
Atlantic	TNA	23.42	8.86	14.98
	TA	12.10	36.05	5.86
	TSA	8.17	5.41	0.19
	STNA	4.68	0.09	1.66
	CARS	0.68	1.60	2.86
	Gulf of Mexico	0.02	0.03	–
Pacific	Total	49.07	52.04	25.55
	TSP	2.00	0.34	28.79
	TNP	0.64	0.42	7.69
	STNP	0.00	0.10	–
Terrestrial	Total	2.64	0.86	36.48
	ORIC	12.80	18.02	11.54
	NAMZ	7.50	5.78	7.54
	SAMZ	0.53	0.26	1.54
	NOSA	9.61	8.08	17.32
	Total	30.44	32.46	37.94
	GUY	3.08	8.42	–
	NEB	0.69	2.53	–
Others	Western Africa	0.42	0.43	–
	TOC	0.33	0.52	–
	PECH	0.23	0.02	–
	Central America	0.09	0.19	–
	LPRB	0.01	0.00	–
	U S	0.01	0.00	–
	Others	12.98	2.53	–
Total	17.84	14.64	–	

expected these variables are in the same range of values (same magnitude order) and similar qualitative behavior. We have not normalized the time series to emphasize how the three methods can be compared in terms of their units.

For Atlantic sources (Fig. 10), during the austral summer season, when the ITCZ is at its southern-most position, the main moisture contribution to NOSA comes from TNA. Both the DRM and FLEXPART show maximum contribution from the TNA during the austral summer. QIBT shows a qualitatively similar behavior but with a smaller contribution. The DRM even shows evidence of moisture coming from as far north as the STNA region during this time (not shown), suggesting long-range cross-equatorial flow (Wang and Fu 2002). As the ITCZ moves northward during the austral fall, the contribution from TNA diminishes and in contrast, moisture inflow from TSA increases and reaches its maximum in August (although FLEXPART shows an

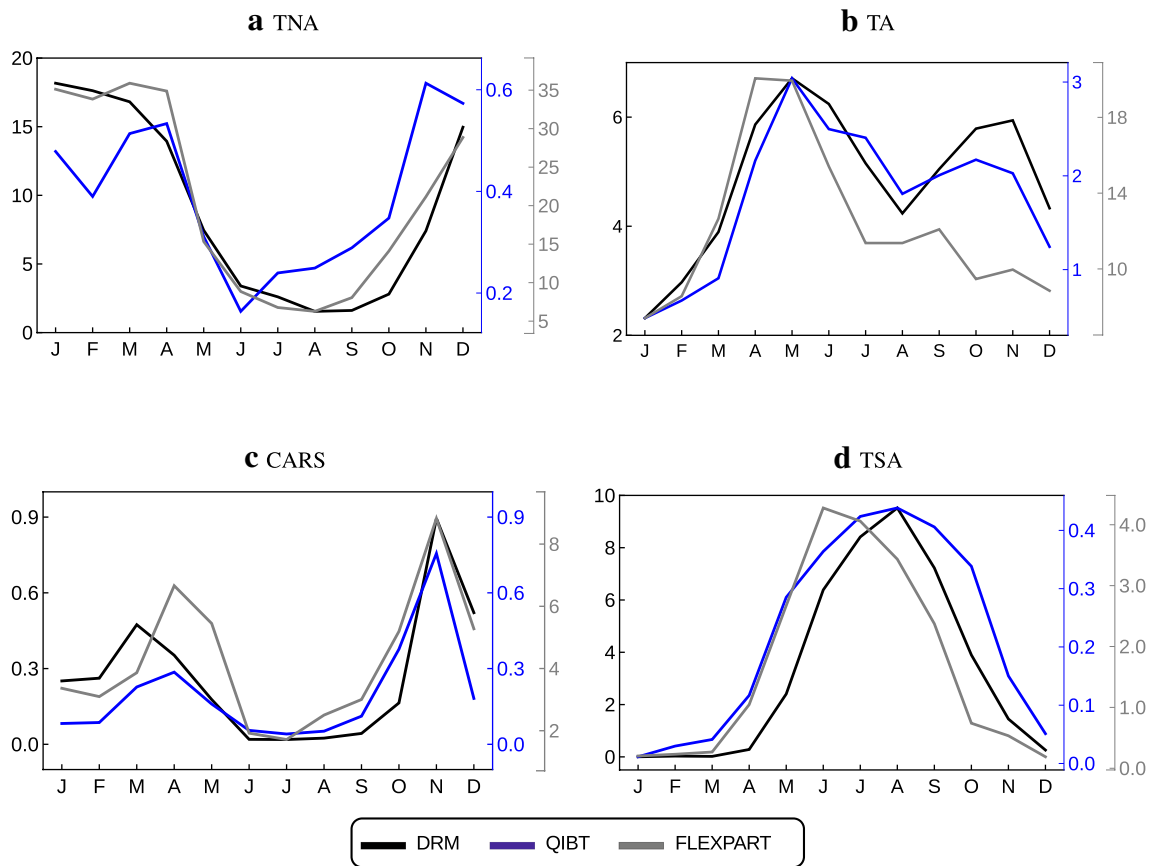


Fig. 10 Precipitable water, evaporative moisture and net moisture lost accounted over NOSA by DRM, QIBT and FLEXPART (forward), respectively, from Atlantic sources. **a** Tropical North Atlantic,

b Tropical Atlantic, **c** Caribbean sea and **d** Tropical South Atlantic. Color in each vertical axis according to the corresponding model. Units in mm/month

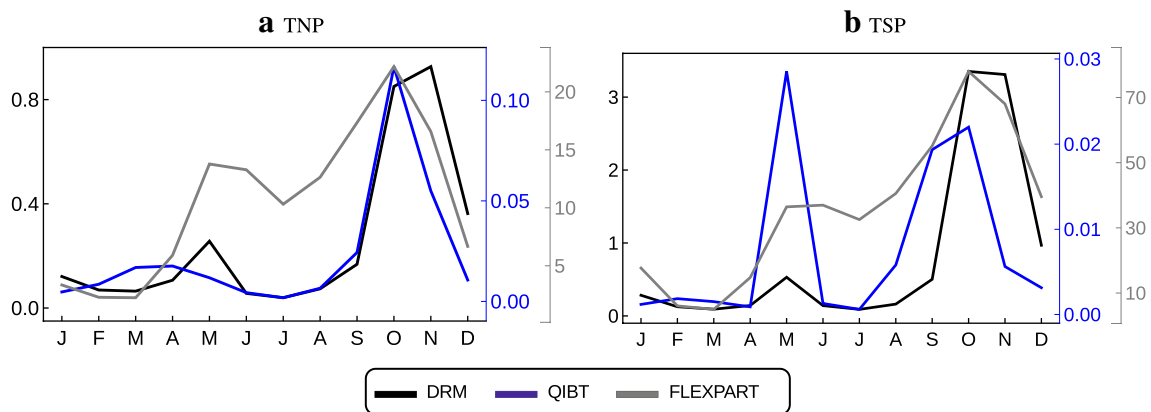


Fig. 11 As Figure 10 but for Pacific sources. **a** Tropical North Pacific. **b** Tropical South Pacific

earlier peak). The TA region behaves as a transition zone between the North and South Atlantic, exhibiting a bimodal regime that coincides with the regional rainy periods (see Sect. 2). The three models also show an important contribution from CARS region, with two noticeable peaks, the

first during the Austral fall and a second higher peak in the transition from spring to summer.

The adjacent Pacific Ocean contributes significantly to the mean total precipitable water (Fig. 11). TNP and TSP feature a bimodal regime of moisture contribution to

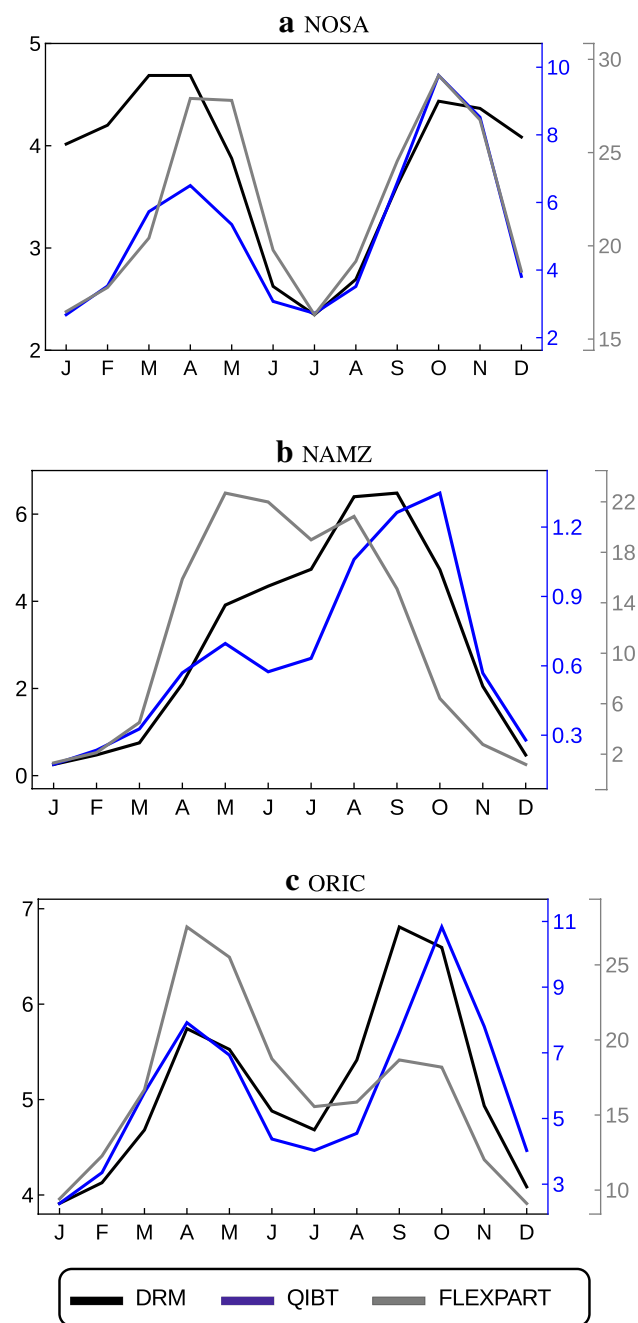


Fig. 12 As Figure 10 but for Terrestrial sources. **a** Northern South America (target region, local recycling). **b** Northern Amazon Basin. **c** Orinoco Basin

NOSA, with one peak during MAM and another during SON. In contributions from TNP, the second peak is higher than the first one for DRM and QIBT models, while FLEXPART shows a smaller difference between both peaks. The monthly amount captured by FLEXPART exceeds in two orders of magnitude what is accounted by DRM and QIBT. This difference can be explained by the vertical integration of the DRM that may underestimate the moisture transport

from the lower troposphere in the Pacific. The underestimation from QIBT is more likely due to the fact that the target region for QIBT is the Magdalena River basin (not the entire NOSA), and the Magdalena basin does not extend to the Pacific coast. The Southern Pacific (TSP) has a considerably higher contribution than TNP, revealing long-range transport into this region. The first peak occurs in May for DRM and QIBT and extends to June in FLEXPART. Contrary to DRM and FLEXPART, in QIBT the first peak is greater than the second one. The three models agree that an important contribution from the adjacent Pacific occurs during the SON season. This feature is associated with a reversal of the zonal component of the mean integrated water vapor (IWT) off the west coasts of northern Colombia (Chocó) and Panama (~ 5°N, Figs. 5, 7). The increase of transport occurs as a result of the strengthening of the westerly flow at low levels, with a maximum near the 925 hPa level off the coast of Colombia and Panama (Poveda et al. 2006; Poveda and Mesa 2000). Note that the westerly flow off the west coast of NOSA provides not only moisture from the adjacent Pacific, but also enhances the convergence of moisture over NOSA when interacting with the easterly flow (Mapes et al. 2003) over north and eastern NOSA (Figs. 5, 7). Such increase in the convergence of moisture is associated with a peak in precipitation (Fig. 3) and precipitable water (Fig. 11a, b).

Terrestrial moisture sources of major contribution to Colombia are the Amazon Basin, Orinoco Basin and local recycling from NOSA (Fig. 12). Terrestrial regions account for roughly 30, 32 and 37% of the total precipitable water into NOSA according to the DRM, QIBT and FLEXPART, respectively. Local recycling (NOSA), which accounts for nearly 10% of the moisture contribution for DRM and QIBT and 17% for FLEXPART shows a bimodal distribution with peaks in March–April, (for FLEXPART the maximum is extended until May) and in October–November during the time of precipitation peak. Contributions from the Orinoco Basin (ORIC) are larger than those from NOSA in QIBT and DRM models, but smaller in FLEXPART (12.80, 18.02 and 11.54% according to DRM, QIBT and FLEXPART), with a similar bimodal distribution, linked to the passage of the ITCZ. Results from DRM and QIBT suggest that the influence of ORIC is higher during austral spring, however FLEXPART reaches the maximum during austral fall. This region is characterized by large wetland areas that remain saturated with water from August to November after the peak of precipitation (Lewis et al. 2000). During this period, soil water is highly available and the evaporative process is strengthened. The seasonal increase of evaporation is captured in FLEXPART with a second peak relatively lower than the first one. In contrast, contributions from NAMZ show a quasi unimodal

distribution with maximum value during different months for each model within the April to November period with a small decrease during June–July (Fig 12). The large contribution from the Amazon corresponds very well to the peak of photosynthetic activity in the Amazon forest from mid May to mid November (Doughty and Goulden 2008) and could be explained by the effect of transpiration from the Amazon rainforest on regional circulation patterns (Makarieva et al. 2013). In general, the results of the three models confirm previous work that highlights regional moisture from Amazon Basin as an important moisture source for the Colombian hydroclimatology and a regional provider of ecosystem services (Poveda et al. 2006; IDEAM 2005). Furthermore, our results also show the importance of the Orinoco River Basin as a moisture source for Colombia.

Figure 13 presents the summary of regional moisture contributions from the three models in terms of percentages of moisture captured from each source region. This is a comparative measurement among the three models, despite the differences inherent to each model, and provides an overview of the relative contributions that each model is able to represent.

3.2 Regional moisture transport by low-level jet systems

The CLLJ is a potential mechanism of moisture transport from the Caribbean and North Tropical Atlantic to NOSA. DRM, QIBT and FLEXPART capture significant moisture contributions from TNA during October to April period, which corresponds with the boreal winter maximum of the CLLJ, but also with the lowest position of the ITCZ. This result suggests that the CLLJ could be working as a mechanism of moisture transport across NOSA (and surrounding areas) that contributes to the development of the South America Summer Monsoon system (Vuille et al. 2012; Zhou and Lau 2001). This also suggests a role of the NOSA area as an important passage of moisture fluxes across the Americas. None of the three models show moisture transport associated with the CLLJ during the boreal summer (Figs. 5, 7). A possible reason is that during this season the NASH is shifted northward, extending toward the northern Caribbean Sea, thus the CLLJ has a preferential influence over Central America (Durán-Quesada et al. 2010).

In agreement with previous work on the CHOCO Jet (Poveda et al. 2006; Poveda and Mesa 2000) we find

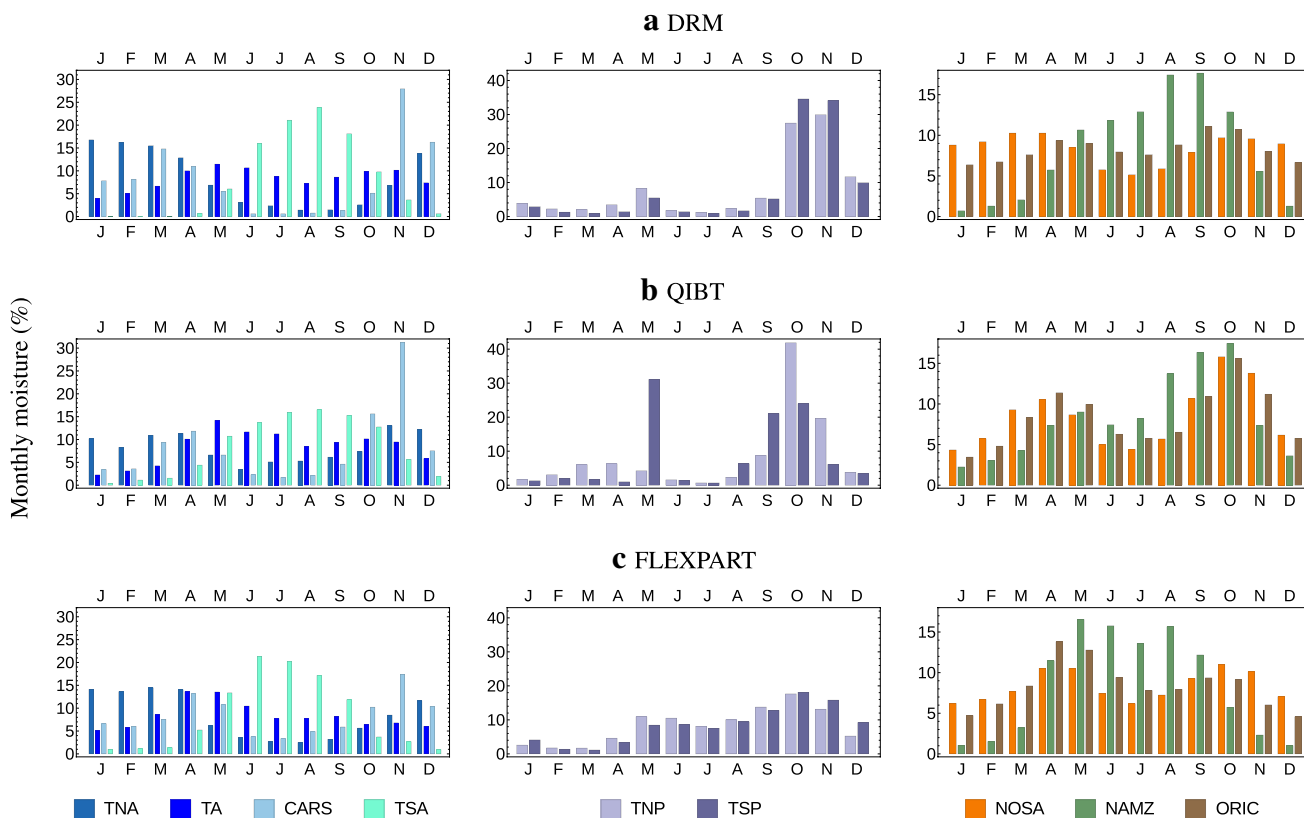


Fig. 13 Percentage of monthly contribution of the multiannual amount captured from each influential source region in NOSA as it is represented by the models **a** DRM, **b** QIBT, **c** FLEXPART. Regions

are shown in *same colors* than in Fig. 9 and grouped by Atlantic (*left*), Pacific (*center*) and Terrestrial (*right*) sources

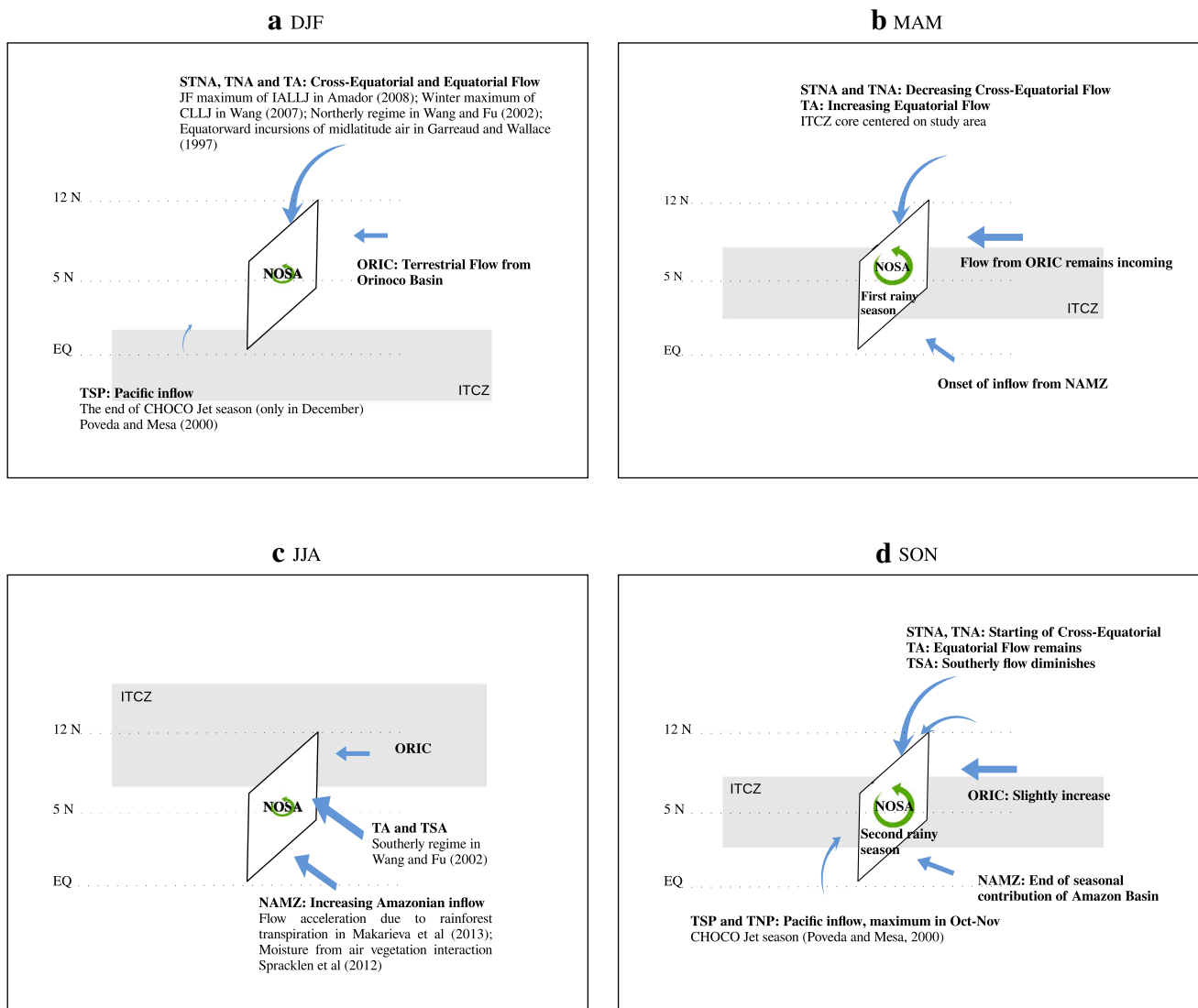


Fig. 14 Qualitative summary of the seasonal progression of moisture source contributions over NOSA common to the three models. Citations appear only when the result has been previously reported. The

relative location of the ITCZ in the study area is in *gray color*. The seasonal intensity of local moisture recycling is represented by the *green arrows*

moisture transport from the Pacific Ocean (TNP and TSP) is mostly active during September to December, with maximum development in October, as shown by DRM, QIBT and FLEXPART models, with a higher contribution from the TSP than the TNP, suggesting long-range moisture transport. The FLEXPART backward simulation (Fig. 6c) shows an extended source of moisture close to the South America coast, following the CHOCO jet trajectory. This pattern is not captured by DRM or QIBT simulations (Fig. 8a, b). We found that the development of the CHOCO Jet is preceded by moisture flux from

the Amazon Basin and the Tropical South Atlantic. As we proposed in Sect. 2.2 (Fig. 6), there is an orographic channel, located in the western border between Ecuador and Perú, that allows the moisture flux from the eastern flank of the Tropical Andes to the Tropical Pacific Ocean region. This flux (which is clearly noticeable during the JJA season, when the regional moisture contributions to NOSA mostly come from NAMZ and TSA), reinforces the convergence of moisture over the northwestern continental margin, and may be considered a contributing factor for the development of the CHOCO Jet system.

4 Concluding remarks

Reanalyses data are an important resource to understand the climate dynamics in areas with sparse observations. Colombia is characterized by a complex terrain that modulates local circulation and thermodynamic processes. Consequently, the representation of regional dynamics constitutes a challenge for reanalyses products. ERA-Interim is particularly useful in regional studies due to its high spatial resolution. Higher resolution allows for a better characterization of the regional topography and more realistic representation of the interaction of atmospheric circulation with the Andes. The present analysis has shown that ERA-Interim realistically captures the spatio-temporal structure of regional moisture processes in the Colombian hydrographic units defined by the largest basins in the country. This is true even in the Caribbean and Pacific basins, which exhibit the largest complexity due to the presence of the three branches of the Colombian Andes and the spatial variability of transport processes. Due to these complexities, precipitation is overestimated by ERA-Interim. However, ERA-Interim's realistic representation of climate processes can be seen in the correlation between the standardized anomalies of the Magdalena River discharges and precipitation estimates from ERA-Interim (Sect. 2, Fig. 4).

Most of the moisture over NOSA accumulates downwind of the mean vertically integrated moisture flux over the Colombian Andes region. Precipitation over this region contributes to the two largest rivers in the country: the Magdalena and Cauca, which run between the three mountain ranges (Fig. 1). Moisture in NOSA is either of local or remote terrestrial origin, or transported from the oceans.

The moisture sources that contribute to precipitation in NOSA are calculated using three different methodologies: DRM, QIBT and FLEXPART. Despite the differences in the methods and input data for QIBT versus DRM and FLEXPART, we have gained an understanding of the seasonal evolution of moisture sources. Figure 14 summarizes the results of features that are commonly captured by the three models. During the Austral Summer (DJF), the ITCZ is at its southern-most position and most of the moisture is coming from the Atlantic (TNA), Caribbean (CARS) and even regions further north (as STNA, not shown here). As the ITCZ moves into northern South America and the first rainy season begins, terrestrial sources from the Orinoco and local recycling become more important, as well as moisture from the Tropical Atlantic (TA). The northern-most position of the ITCZ (JJA) corresponds to strong contributions from the Amazon basin and the Tropical South Atlantic (TSA). During the Austral spring (SON—corresponding to the second passage of the ITCZ through northern South America), local recycling and moisture from the Orinoco are again important, while the contribution from

the Amazon decreases. During this season, particularly during October and November, the adjacent Pacific (TSP and TNP) becomes an important contributor to the Western coast of NOSA via the CHOCO jet. The pattern summarized in Figs. 13 and 14 is in agreement with previous findings by Sakamoto et al. (2012) and Arias et al. (2015) from analyses of shorter periods. In the present work, the seasonal evolution of moisture sources emerges as a robust signature observed in three different transport models from multidecadal calculations, however there are limitations in the spatial representation of regional atmospheric transport due to the restricted resolution to represent the steep regional topography in the three models.

Finally, terrestrial sources play an important role as sources of moisture for Colombia—highlighting the regional sensitivity to surface processes. This could potentially have implications related to changes in vegetation and land cover uses that directly affect transpiration and atmospheric circulation.

Acknowledgements This research has been supported by the USAID-NSF PEER program (Cycle 1, project 31) and the Universidad de Antioquia through its programs CODI (*Convocatoria Programática 2013*, Project PRG 13-2-03), Project PI12-1-03 and Fondo de Pasajes Internacionales. Isabel Hoyos is also supported by the Programa Enlazamundos from Alcaldía de Medellín. Francina Domínguez is funded by NSF award AGS 1045260. Raquel Nieto and Luis Gimeno acknowledge funding by the Spanish MINECO and FEDER within the project TRAMO. Raquel Nieto is also supported by the CNPq Grant 314734/2014-7 by the Brazilian Government. The TRMM data used in this study were acquired as part of the Tropical Rainfall Measuring Mission (TRMM). The algorithms were developed by the TRMM Science Team. The data were processed by the TRMM Science Data and Information System (TSDIS) and the TRMM office; they are archived and distributed by the Goddard Distributed Active Archive Center. TRMM is an international project jointly sponsored by the Japan National Space Development Agency (NASDA) and the US National Aeronautics and Space Administration (NASA) Office of Earth Sciences. The authors thank the valuable comments and suggestions of the anonymous reviewers that greatly improve the final version of the paper.

References

- Amador JA (2008) The intra-Americas sea low-level jet. *Ann N Y Acad Sci* 1146(1):153188. doi:[10.1196/annals.1446.012](https://doi.org/10.1196/annals.1446.012)
- Andersson E, Bauer P, Beljaars A, Chevallier F, Hólm E, Janisková M, Källberg P, Kelly G, Lopez P, McNally A, Moreau E, Simmons AJ, Thépaut JN, Tompkins AM (2005) Assimilation and modeling of the atmospheric hydrological cycle in the ECMWF forecasting system. *Bull Am Meteorol Soc* 86(3):387–402. doi:[10.1175/bams-86-3-387](https://doi.org/10.1175/bams-86-3-387)
- Arias PA, Martínez JA, Vieira SC (2015) Moisture sources to the 2010–2012 anomalous wet season in northern South America. *Clim Dyn*. doi:[10.1007/s00382-015-2511-7](https://doi.org/10.1007/s00382-015-2511-7)
- Bass MS, Finer M, Jenkins C, Clinton N, Kreft H, Cisneros-Heredia DF, McCracken SF et al (2010) Global conservation significance of Ecuador's Yasuní National Park. *PLoS One* 5(1):e8767. doi:[10.1371/journal.pone.0008767](https://doi.org/10.1371/journal.pone.0008767)

- Bhushan S, Barros AP (2007) A numerical study to investigate the relationship between moisture convergence patterns and orography in central Mexico. *J Hydrometeorol* 8(6):1264–1284. doi:10.1175/2007JHM791.1
- Burde GI, Zangvil A (2001) The estimation of regional precipitation recycling. Part I: review of recycling models. *J Climate* 14(12):2497–2508. doi:10.1175/1520-0442(2001)014<2497:teorpr>2.0.co;2
- Buytaert W, Bièvre BD (2012) Water for cities: the impact of climate change and demographic growth in the tropical Andes. *Water Resour Res* 48(8):1–13
- Carvajal YE, Jiménez HE, Materón HM (1998) Incidencia del fenómeno del Niño en la hidroclimatología del valle del río Cauca-Colombia. *B Inst Fr Étud Andines* 27(3):743–751
- Céleri R, Feyen J (2009) The hydrology of tropical Andean ecosystems: importance, knowledge status, and perspectives. *Mount Res Dev* 29(4):350–355
- Dee D, Uppala S, Simmons A, Berrisford P, Poli P, Kobayashi S, Andrae U, Balmaseda M, Balsamo G, Bauer P et al (2011) The ERA-Interim reanalysis: Configuration and performance of the data assimilation system. *Q J R Meteorol Soc* 137(656):553–597
- Dirmeyer PA, Brubaker KL (1999) Contrasting evaporative moisture sources during the drought of 1988 and the flood of 1993. *J Geophys Res* 104(D16):19383–19397. doi:10.1029/1999jd900222
- Dirmeyer PA, Brubaker KL (2007) Characterization of the global hydrologic cycle from a back-trajectory analysis of atmospheric water vapor. *J Hydrometeorol* 8(1):20–37. doi:10.1175/jhm557.1
- Dominguez F, Kumar P, Liang XZ, Ting M (2006) Impact of atmospheric moisture storage on precipitation recycling. *J Clim* 19(8):1513–1530
- Doughty CE, Goulden ML (2008) Seasonal patterns of tropical forest leaf area index and CO₂ exchange. *J Geophys Res*. doi:10.1029/2007jg000590
- Durán-Quesada A, Reboita M, Gimeno L (2012) Precipitation in tropical America and the associated sources of moisture: a short review. *Hydrol Sci J* 57(4):612–624
- Durán-Quesada AM, Gimeno L, Amador J, Nieto R (2010) Moisture sources for Central America: identification of moisture sources using a lagrangian analysis technique. *J Geophys Res Atmos* (1984–2012) 115(D5):1–15
- Eslava (1994) *Climatología del Pacífico Colombiano*, 1st Ed. Academia Colombiana de Ciencias Geofísicas. Santafé de Bogotá D.C
- Garreaud R (2009) The Andes climate and weather. *Adv Geosci* 22(22):3–11. doi:10.5194/adgeo-22-3-2009
- Geer AJ, Bauer P, Lopez P (2008) Lessons learnt from the operational 1D + 4D-var assimilation of rain- and cloud-affected SSM/I observations at ECMWF. *QJR Meteorol Soc* 134(635):1513–1525. doi:10.1002/qj.304
- Hartmann DL (1994) *Global Physical Climatology* (International Geophysics). Academic. San Diego, California
- Hastings DA, Dunbar PK (1998) Development and assessment of the Global Land One-km Base Elevation Digital Elevation Model (globe). *Int Arch Photogramm Remote Sens Spat Inf Sci* 32(4):218–221
- Hoyos I, Baquero-Bernal A, Jacob D, Rodríguez BA (2013) Variability of extreme events in the Colombian Pacific and Caribbean catchment basins. *Clim Dyn* 40(7–8):1985–2003. doi:10.1007/s00382-012-1487-9
- Hoyos I, Baquero-Bernal A, Hagemann S (2013) How accurately are climatological characteristics and surface water and energy balances represented for the Colombian Caribbean Catchment Basin? *Clim Dyn* 41(5–6):1269–1290. doi:10.1007/s00382-013-1685-0
- Hoyos I, Arenas-Suárez T, Martínez JA, Rodríguez B (2014) Which climate traits can and cannot be represented by reanalyses and reconstructed data sets over Colombia? In: LOTRED-SA 3rd International Symposium Climate change and human impact in central and South America over the last 2000 years Observations and Models. <http://www.pages-igbp.org/download/docs/meeting-products/abstracts/2014-lotred-medellin.pdf>. Accessed 15 Feb 2017
- IDEAM (2005) *Atlas climatológico de Colombia*. Instituto de Hidrología, Meteorología y Estudios Ambientales de Colombia, República de Colombia. ISBN:958-8067-14-6
- Jackson RB, Carpenter SR, Dahm CN, McKnight DM, Naiman RJ, Postel SL, Running SW (2001) Water in a changing world. *Ecol Appl* 11(4):1027–1045. doi:10.1890/1051-0761(2001)011[1027:WIACW]2.0.CO;2
- Kanamitsu M, Ebisuzaki W, Woollen J, Yang SK, Hnilo JJ, Fiorino M, Potter GL (2002) Ncepdoe AMIP-ii reanalysis (r-2). *Bull Am Meteorol Soc* 83(11):1631–1643. doi:10.1175/bams-83-11-1631
- Lewis WM, Hamilton SK, Lasi MA, Rodriguez M III, JFS, (2000) Ecological determinism on the orinoco floodplain. *BioScience* 50(8):681–692. doi:10.1641/0006-3568(2000)050[0681:EDOT]2.0.CO;2
- Lin YL, Chiao S, Wang TA, Kaplan ML, Weglarz RP (2001) Some common ingredients for heavy orographic rainfall. *Weather Forecast* 16(6):633–660. doi:DOIurl10.1175/1520-0434(2001)016<0633:SCIFHO>2.0.CO;2
- López ME, Howell WE (1967) Katabatic winds in the equatorial Andes. *J Atmos Sci* 24(1):29–35. doi:10.1175/1520-0469(1967)024<0029:KWITEA>2.0.CO;2
- Lorenz C, Kunstmann H (2012) The hydrological cycle in three state-of-the-art reanalyses: Intercomparison and performance analysis. *J Hydrometeorol* 13(5):1397–1420. doi:10.1175/jhm-d-11-088.1
- Makarieva AM, Gorshkov VG, Sheil D, Nobre AD, Li BL (2013) Where do winds come from? a new theory on how water vapor condensation influences atmospheric pressure and dynamics. *Atmos Chem Phys* 13(2):1039–1056. doi:10.5194/acp-13-1039-2013
- Mapes BE, Warner TT, Xu M, Negri AW (2003) Diurnal patterns of rainfall in northwestern South America. part I: Observations and context. *Mon Weather Rev* 131(5):799–812. doi:10.1175/1520-0493(2003)131<0799:DPORIN>2.0.CO;2
- Martínez JA, Dominguez F (2014) Sources of atmospheric moisture for the La Plata river Basin. *J Clim* 27(17):6737–6753. doi:10.1175/jcli-d-14-00022.1
- Mesa O, Poveda G, Carvajal L (1997) *Introducción al clima de Colombia*. Universidad Nacional. Santafé de Bogotá, D.C
- Montgomery DR, Balco G, Willett SD (2001) Climate, tectonics, and the morphology of the Andes. *Geology* 29(7):579–582. doi:10.1130/0091-7613(2001)029<0579:CTATMO>2.0.CO;2
- Muñoz E, Busalacchi AJ, Nigam S, Ruiz-Barradas A (2008) Winter and summer structure of the caribbean low-level jet. *J Clim* 21(6):1260–1276. doi:10.1175/2007jcli1855.1
- Myers N, Mittermeier RA, Mittermeier CG, Da Fonseca GA, Kent J (2000) Biodiversity hotspots for conservation priorities. *Nature* 403(6772):853–858. doi:10.1038/35002501
- Numaguti A (1999) Origin and recycling processes of precipitating water over the eurasian continent: experiments using an atmospheric general circulation model. *J Geophys Res* 104(D2):1957. doi:10.1029/1998jd200026
- Pabón J (2003) El cambio climático global y su manifestación en Colombia. *Cuadernos Geografía* 12:111–119
- Pabón J, Eslava J, Gómez R (2001) Generalidades de la distribución espacial y temporal de la temperatura del aire y de la precipitación en Colombia. *Meteorología Colombiana* 4:47–59
- Poveda G, Mesa OJ (2000) On the existence of Lloró (the rainiest locality on Earth): Enhanced ocean-land-atmosphere interaction by a low-level jet. *Geophys Res Lett* 27(11):1675–1678. doi:10.1029/1999GL006091

- Poveda G, Waylen PR, Pulwarty RS (2006) Annual and inter-annual variability of the present climate in northern South America and southern Mesoamerica. *Palaeogeogr Palaeoclimatol Palaeoecol* 234(1):3–27. doi:[10.1016/j.palaeo.2005.10.031](https://doi.org/10.1016/j.palaeo.2005.10.031)
- Poveda G, Jaramillo L, Vallejo LF (2014) Seasonal precipitation patterns along pathways of south american low-level jets and aerial rivers. *Water Resour Res* 50(1):98–118. doi:[10.1002/2013WR014087](https://doi.org/10.1002/2013WR014087)
- Roe GH (2005) Orographic precipitation. *Annu Rev Earth Planet Sci* 33:645–671. doi:[10.1146/annurev.earth.33.092203.122541](https://doi.org/10.1146/annurev.earth.33.092203.122541)
- Sakamoto MS, Ambrizzi T, Poveda G (2012) Moisture sources and life cycle of convective systems over Western Colombia. *Adv Meteorol* 2011:1–11. doi:[10.1155/2011/890759](https://doi.org/10.1155/2011/890759)
- Snow JW (1976) The climate of northern South America. In: Schwedtfeger W (ed) *Climates of Central and South America*, World Survey of Climatology, vol 12. Elsevier Scientific Publishing Co, Amsterdam, pp 295–403
- Stohl A, James P (2004) A lagrangian analysis of the atmospheric branch of the global water cycle. part I: Method description, validation, and demonstration for the (August 2002) Flooding in central Europe. *J Hydrometeorol* 5(4):656–678. doi:[10.1175/1525-7541\(2004\)005<0656:alaota>2.0.co;2](https://doi.org/10.1175/1525-7541(2004)005<0656:alaota>2.0.co;2)
- Stohl A, Forster C, Frank A, Seibert P, Wotawa G (2005) Technical note: The lagrangian particle dispersion model FLEXPART version 6.2. *Atmos Chem Phys* 5(9):2461–2474. doi:[10.5194/acp-5-2461-2005](https://doi.org/10.5194/acp-5-2461-2005)
- Tavolato C, Isaksen L (2010) Data usage and quality control for ERA-40, ERA- Interim, and the operational ECMWF data assimilation system. ERA Report Series 7, ECMWF, Reading
- Trenberth KE, Fasullo JT, Mackaro J (2011) Atmospheric moisture transports from ocean to land and global energy flows in reanalyses. *J Clim* 24(18):4907–4924. doi:[10.1175/2011jcli4171.1](https://doi.org/10.1175/2011jcli4171.1)
- Uppala SM, Kälberg PW, Simmons AJ (2005) The era-40 re-analysis. *Q J R Meteorol Soc* 131(612):2961–3012. doi:[10.1256/qj.04.176](https://doi.org/10.1256/qj.04.176)
- Vuille M, Burns SJ, Taylor BL, Cruz FW, Bird BW, Abbott MB, Kanner LC, Cheng H, Novello VF (2012) A review of the South American monsoon history as recorded in stable isotopic proxies over the past two millennia. *Clim Past* 8(4):1309–1321. doi:[10.5194/cp-8-1309-2012](https://doi.org/10.5194/cp-8-1309-2012)
- Wagener T, Sivapalan M, Troch P, McGlynn B, Harman C et al (2010) The future of hydrology: An evolving science for a changing world. *Water Resour Res*. doi:[10.1029/2009WR008906](https://doi.org/10.1029/2009WR008906)
- Wang C (2007) Variability of the caribbean low-level jet and its relations to climate. *Clim Dyn* 29(4):411–422. doi:[10.1007/s00382-007-0243-z](https://doi.org/10.1007/s00382-007-0243-z)
- Wang C, Lee SK (2007) Atlantic warm pool, caribbean low-level jet, and their potential impact on atlantic hurricanes. *Geophys Res Lett*. doi:[10.1029/2006gl028579](https://doi.org/10.1029/2006gl028579)
- Wang H, Fu R (2002) Cross-equatorial flow and seasonal cycle of precipitation over South America. *J Clim* 15(13):1591–1608. doi:[10.1175/1520-0442\(2002\)015<1591:cefasc>2.0.co;2](https://doi.org/10.1175/1520-0442(2002)015<1591:cefasc>2.0.co;2)
- Waylen PR, Poveda G (2002) El Niño-Southern Oscillation and aspects of western South America hydro-climatology. *Hydrol Process* 16(6):1247–1260. doi:[10.1002/hyp.1060](https://doi.org/10.1002/hyp.1060)
- Zhou J, Lau KM (2001) Principal modes of interannual and decadal variability of summer rainfall over South America. *Int J Climatol* 21(13):1623–1644. doi:[10.1002/joc.700](https://doi.org/10.1002/joc.700)